Chapter 10

Surface-Modified Graphene for Mid-Infrared Detection

Mehrdad Siahsar, Mahboubeh Dolatyari,
Ali Rostami and Ghasem Rostami

Additional information is available at the end of the chapter

http://dx.doi.org/10.5772/67490

Abstract

In this chapter, morphology variation and electronic structure in a surface-modified graphene are demonstrated by both calculation and experimental results. The results indicate that the band structure and morphology of modified graphene sheets are altered because of changing in the type of hybridization of carbon atoms in the graphene sheet. Accordingly, the band gap of graphene can be tuned by surface modification using organic molecules. Then, modified graphene is used for fabrication of infrared detectors. The properties of unmodified graphene photodetectors were also measured so as to compare with modified graphene photodetectors. The results demonstrate that modification of graphene using organic ligands improved the detection parameters such as fast response time, electrical stability and low dark current. Moreover, the sensitivity of photodetectors based on modified graphene was significantly improved.

Keywords: fabrication, photodetector, organic ligand, modified, unmodified, IR, graphene

1. Introduction

Graphene is a two-dimensional sp^2-bonded carbon atom on a honeycomb lattice [1]. The particular arrangement of carbon atoms in graphene leads to a novel energy dispersion relation, mean root of the appealing electronic characteristic, which corresponds to massless fermions [2–4]. In spite of the fact that graphene has much favourable properties, which have revolutionized the miscellaneous aspects of science and technology, it could not be an applicable material for special purposes because of its shortcomings that have to be overcome [5]. Although, in the last decade, the unique properties of graphene, namely electronic, mechanical, optical and chemical properties, and its possible applications have been widely investigated, the

absence of a gapped semiconductor with properties like that of graphene is strongly felt, especially in the graphene-based photodetectors which do not enjoy fast response time stemming from zero band gap of graphene [6–18]. In addition, another salient weakness of graphene's application appears in the designing of transistor-based digital circuits [19]. Transistor made by graphene, in the off-state, has a current due to minimum conductivity of graphene [19]. Accordingly, the power consumption of fabricated circuits is considerable. The engineering of band structure of graphene sheet has been extensively studied. Band gap about 0.5 eV can be formed in nanoribbons with the width about 10 nm [20–22]. In this method, controling the value of band gap which is strongly affected by the structure of nano ribbons edges is difficult. Moreover, bilayer graphene can be used for this purpose, which is synthesized with difficulty [23, 24]. One can manipulate electrical and magnetic properties of graphene by introducing different defect state in graphene [25, 26]. Because all atoms are placed on the surface of graphene, density of electrons is high on it, so active is the graphene sheet that it can easily react with the gases in the surrounding atmosphere. Therefore, the chemical instability of graphene leads to use vacuum condition in order to obtain repetitive results.

Some ideas have been investigated so as to overcome the mentioned weaknesses. By studying the electron transport properties of graphene-like two-dimensional materials, one can reach to this result that using heterostructures of graphene and other two-dimensional materials have significant impact on the application of graphene [5, 27–32]. Instead of two-dimensional materials, zero- and one-dimensional organic or inorganic materials can be used in the above-mentioned heterostructures [33–36]. A focal point in this research is modification of the surface of the graphene sheet via zero-dimensional organic ligands. In order to realize the process of modification of graphene sheet, it is important to know that by adding hydrogen to the surface of graphene sheet, which is highly conducting, it could be converted into a novel material known as graphane, two-dimensional hydrocarbon, which is an insulator with direct band gap of 3.7 eV [37]. The alteration in the percentage of hydrogenation of graphene can lead to the creation of various band gap. In other words, the engineering of band gap synthesized can be possible by hydrogenation from zero in the graphene to 3.7 eV in the fully hydrogenated graphene [37]. This achievement should broaden the spectrum of photonics application of graphene.

To modify surface of graphene sheet, we introduce trap states and a band gap in graphene by means of organic ligands, which interact with graphene for fabricating sensitive infrared detector operated at 3–5 μm [38–40]. To achieve this, our focus is oriented to the analysis of altered structural arrangement of the organic ligands/graphene with strong interaction between them. Our analysis show that the geometry of synthesized material is affected by the adsorption of organic ligands on graphene layer, for the carbon atoms of graphene strongly interact with the hydrogen atoms of organic ligands. Not only was the structural analysis of the synthesized materials operated, but calculation of the band structure and electron density difference were also calculated to confirm the claim made about modified form of graphene layer.

X-ray diffraction (XRD), atomic force microscope (AFM), scanning electron microscope (SEM), transmission electron microscope (TEM) and electrical resistivity analysis are used to investigate the structure and morphology of the graphene sheets, which were modified by

http://dx.doi.org/10.5772/67490

different concentration of various organic ligands. Finally, we used the synthesized materials as an active layer of metal-graphene-metal (MGM) photodetectors. The experimental investigations show that the detection parameter of fabricated photodetectors improved significantly, for example, temporal time of fabricated photodetectors in our reported work is up to 1000 times faster than the photodetector reported by Yu and co-workers [41].

2. Experimental

2.1. Synthesis and modification

In existance of all fabrication methods of graphene oxide, we prefer to use the following method because the synthesis route plays an important role on the chemical, optical and electrical properties of graphene oxide [42]. Graphite oxide (GO) was synthesized by natural graphite by Hummers' method [43]. A colloidal suspension of synthesized graphene oxide in purified water was prepared by sonication of GO in water (3 mg/mL) for 3 h. Hydrazine monohydrate (1 mL for 3 mg of GO, 98%, Aldrich) was subsequently added to the suspension, in order to remove oxygen components by the hydrazine reduction [38–40]. Additional stirring in an oil bath held at 80°C for 12 h yielded a black precipitation of reduced graphene oxide powder. The obtained materials were centrifuged by water for several times. The synthesized material was dried at 100°C and used for further characterizations and treatment. Organic ligands—thiosemicarbazide, thiophene-2-arbaldehyde, thiophene-2-carboxylic acid and pyridine-4-carboxylic acid—were utilized to modify graphene surface. To prepare modifying organic ligands, 0.5 mg of thiophene-2-arbaldehyde, thiophene-2-carboxylic acid and pyridine-4-carboxylic acid was separately solved in 50 mL water. Moreover, 5 and 10 mg of thiosemicarbazide were independently solved in 7 mL ethanol. Each of the prepared suspension solely was added to a suspension, which consisted of 27 mg of obtained graphene and 30 mL of deionized water. All of the obtained suspensions were stirred for 24 h at room temperature. After purification, the obtained materials were individually added to 30 mL deionized water and dispersed until a thin sheet was formed on top of the colloidal suspension [38–40].

2.2. Fabrication of photodetector

The sheet was transferred on the interdigitated Copper (Cu) contact, which is deposited on a fibre-glass substrate having fingers with a length of 0.5 cm, a width of 150 μm and a pitch of 150 μm. The thickness of the Cu layer was 500 nm [38–40].

2.3. Characterization

In this chapter, all structural characterization and measurement were performed by the following devices:

The crystal structure of modified and unmodified graphene was characterized by powder X-ray diffraction (PXRD) on a Siemens D500 using Cu-kα radiation (λ = 1.541 Å). Ultrasound radiation was performed using UP400s Germany (0.3 cm diameter Ti horn, 200 W, 24 kHz).

The surface morphology of synthesized materials was obtained on a Dual-scope C26 scanning probe and microscope DME atomic force microscope (AFM). The morphology of products was studied via a Tescan model MIRA3 field-emission scanning electron microscope with an accelerating voltage of 10 kV. TEM images were obtained on a Zeiss-EM10C-80KV transmission electron microscope with an accelerating voltage of 80 kV [38–40].

2.4. Computational details

Both the electronic band structure and density of states (DOS) of graphene were calculated by DFT. Calculations were carried out with the CASTEP code using local density approximation (LDA) and the non-local gradient-corrected exchange-correlation functional as parameterized by the Perdew-Zunger scheme (CA-PZ), which uses a plane wave basis set for the valance electrons and ultra-soft pseudo potential for the core electrons. The number of plane waves included in the basis was determined by cut-off energy (Ec) of 300.0 eV. The summation over the Brillouin zone was operated with a *k*-point sampling using a Monkhorst-Pack grid with parameters of 3 × 3 × 1 [40].

3. Results

3.1. Sensitivity

Achilles heel of the current generation of graphene-based photodetectors is their very poor sensitivity. This issue is addressed by adding organic ligands, which introduce band gap. Adjusting the created band gap leads to reduce the dark current, a parameter which plays an absolutely important role in determining sensitivity. The effect of almost all of the organic ligands, which are used to modify graphene sheet, is clear in the improvement of the sensitivity of fabricated photodetectors. A schematic of fabricated photodetector is represented in **Figure 1**.

As shown in **Table 1**, the measured sensitivity, which is calculated by $(R_d - R_i)/R_i$ where R_d and R_i are electrical resistance under dark and infrared light illumination condition, for graphene-based photodetector is 0.5 [38]. Whereas, the sensitivity of photodetectors based on graphene fabricated by Hwang and co-workers, in the highest applied voltage (0.1 V), is 0.5, which is in good agreement with the sensitivity of our fabricated unmodified graphene-based detector [17, 40]. The sensitivity has been boosted by using of back gate. Because of that the applied voltage excites the surface plasmon polariton. Therefore, one outcome of this excitation is enhancement of the sensitivity up to two orders of magnitude [40, 44]. This means the sensitivity can reach to 1. In this case, the sensitivity of the detector is three times less than our modified detector (this can be adjusted by kind of applied organic ligands). In addition, another method to improve sensitivity has been introduced as graphene/silicon-heterostructure [29]. In this condition, the highest sensitivity cannot reach to 1. Using quantum dots is the other way to achieve this goal. Quantum dots (which decorate the graphene sheet) as a zero-dimensional materials significantly affect the sensitivity. This factor can be changed with regard to the types of quantum dots [35]. That nanorods as one-dimensional materials have significant effect on improving the sensitivity of fabricated detectors is an undeniable effect [33].

http://dx.doi.org/10.5772/67490

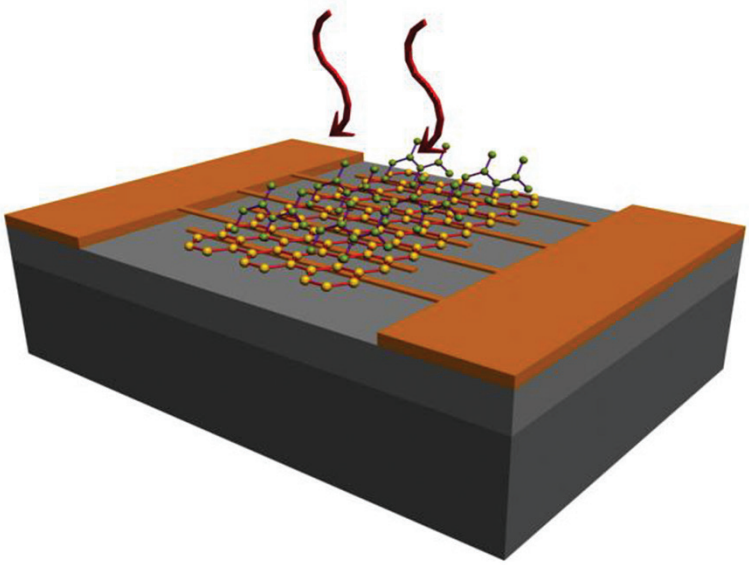

Figure 1. Scheme of fabricated photodetector [40].

Modification of graphene surface by organic ligands such as hydrazine, thiophene-2-carboxylic acid and low-dose thiosemicarbazide increases the sensitivity up to about 1. The sensitivity for photodetector modified by pyridine-4-carboxylic acid is 1.5, which is three times better. Finally, the best ligand in order to improve the sensitivity is high-dose thiosemicarbazide, which causes 500% improvement in the sensitivity compared with unmodified graphene [38–40].

Absorption spectrum of thiophene-2-caboxylic acid, thiophene-2-carbaldehyde and pyridine-4-carboxylic acid has been reported in reference [39]. One possible justification for the

Organic ligand	Sensitivity	Responsivity (A/W)	Rise time (ms)
Unmodified graphene	0.5	10	50
Hydrazine	0.9	14	35
Thiophene-2-carbaldehyde	0.092	0.1	40
Thiophene-2-carboxylic acid	0.9	20	---
Pyridine-4-carboxylic acid	1.5	2.5	38
High-dose thiosemicarbazide	3	9	18
Low-dose thiosemicarbazide	1	10	40

Table 1. Sensitivity, responsivity and rise time of fabricated detectors.

considerable value of photoresponsivity of fabricated photodetector, which was modified with thiophene-2-carboxylic acid is that mentioned ligand has strong absorption in 3–5 μm (2000–3300 cm^{-1}) range [39]. Not only does graphene sheet absorb the IR light, tiophene-2-carboxylic acid ligand absorbs the IR light as well. Consequently, the responsivity of considered detector modified with thiophene-2-carboxylic acid is higher than other fabricated photodetectors [40]. Besides, the devices discussed were stable at room temperature for many days and represented some characteristics during repeated measurement [45].

3.2. I-V characteristic

Figure 2 shows the bias dependence of the I-V characteristic of modified and unmodified graphene-based fabricated photodetectors, which were recorded between 0 and 4 V with voltage steps of 0.1 V. As shown in **Figure 2**, the photo-responsivity ascends with increasing the bias voltage. As stated in **Table 1**, the photo-responsivity value of 10 A/W is observed for detector fabricated by unmodified graphene [39]. Thiosemicarbazide organic ligands do not have remarkable effect on photo-responsivity [40]. The responsivity of fabricated detector is augemented 40% (14A/W) by using hydrazine ligands [38]. By applying thiophene-2-carboxylic acid ligand, one can significantly raise the parameter of photodetector up to 20 A/W [39]. On the other hand, some organic ligands can decrease the mentioned parameter up to 0.1 A/W [39].

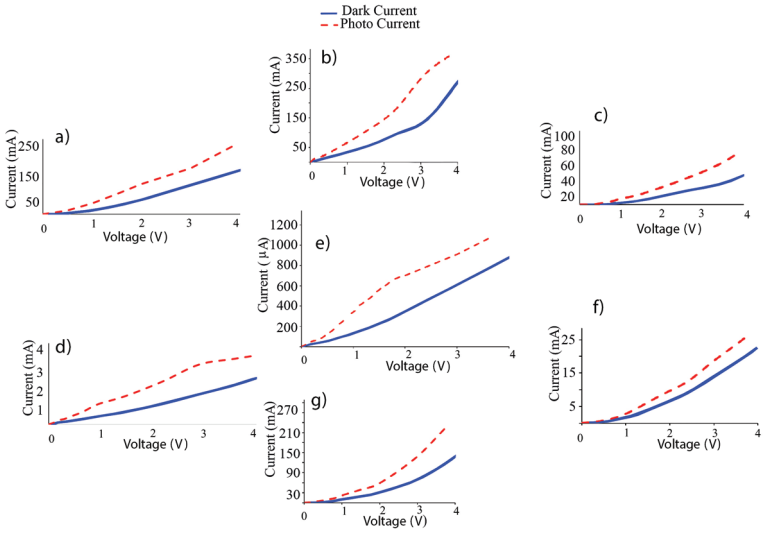

Figure 2. Current-voltage characteristics of fabricated detector based on (a) unmodified grapheme, (b) modified by hydrazine, (c) modified by mercapto acetic acid, (d) modified by low dose thiosemicarbazide, (e) modified by high-dose thiosemicarbazide, (f) modified by thiophene-2-carbaldehyde and (g) modified by thiophene-2-carboxylic acid under illumination of 3–5 μm infrared light [38–40].

http://dx.doi.org/10.5772/67490

3.3. Response time

Figure 3 shows the response time of photodetectors under illumination of IR lamp. The rise time of photodetector based on unmodified graphene is 50 ms [39]. Except fabricated detector based on graphene modified with thiophene-2-carboxylic acid which was too slow to record rise time, all suggested photodetectors based on modified graphene have similar rise time in comparison with photodetectors based on unmodified graphene [38–40]. Among all mentioned photodetectors, photodetector fabricated by graphene which was modified by high-dose thiosemicarbazide is the fastest with the rise time of 18 ms [40]. **Figure 3** shows the response time of investigated photodetectors. All measurements were performed under the illumination of IR lamp with power of 0.1 W in the wavelength range 3–5 μm at room temperature [38–40].

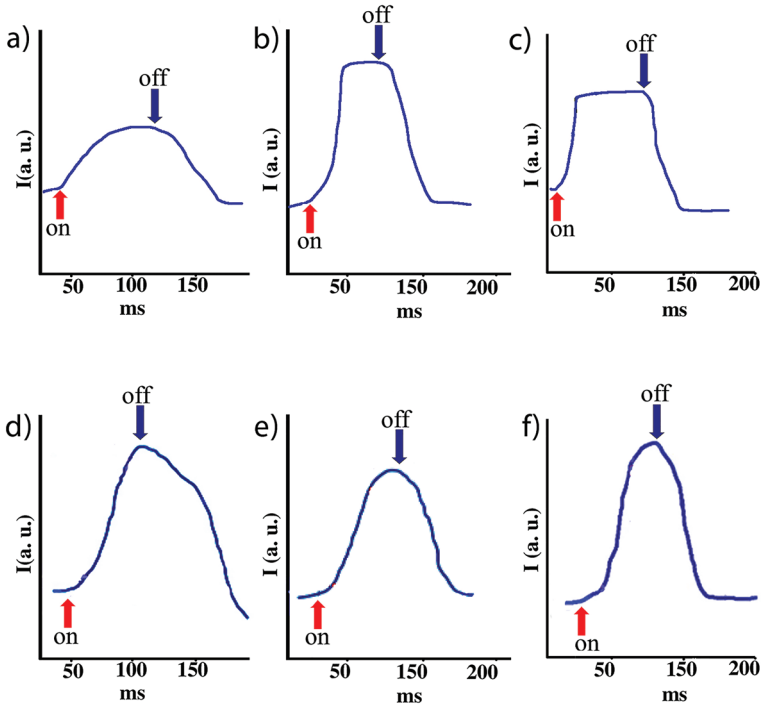

Figure 3. The response time of fabricated detector based on (a) unmodified graphene, (b) modified by low-dose thiosemicarbazide, (c) modified by high-dose thiosemicarbazide, (d) modified by thiophene-2-carbaldehyde, (e) modified by pyridine-4-carboxylic acid and (f) modified by hydrazine [38–40].

3.4. SEM

Figure 4 shows the SEM images of unmodified and modified graphene sheets. It is obvious, from the **Figure 4**, that the graphene sheets are bended in the course of modification process [40]. This phenomenon is in accordance with the calculated result [40]. We attribute the

bending process of the graphene sheets to breaking of the translational symmetry of C-C sp^2 bond after the formation of C-H sp^3 bonds [45]. As shown in **Figure 5**, when hydrogen atoms attach to graphene, carbon atoms move out of plane. Therefore, the graphene sheets bend [45]. One can control the rate of bending of sheets not only by type but also by applying different dose of the organic ligands. As illustrated in **Figure 4**, the synthesized unmodified graphene exhibits almost long and uniform layer. The graphene modified by pyridine-4-carboxylic acid consists of nanosheets with their sizes in about micrometres. However, modification of the graphene using thiophene-2-carboxylic acid leads rolling of micro-sized sheets and forms the flake-like nanorods. One salient example of controlling of bending process via changing the dose of organic ligands is applying different dose of thiosemicarbazide so as to modify graphene sheet [40]. It is obvious that when the dose of thiosemicarbazide is low, sheets will be bended and nanobelts were synthesized. Sheets will be rolled completely, whenever high dose of thiosemicarbazide is applied [40].

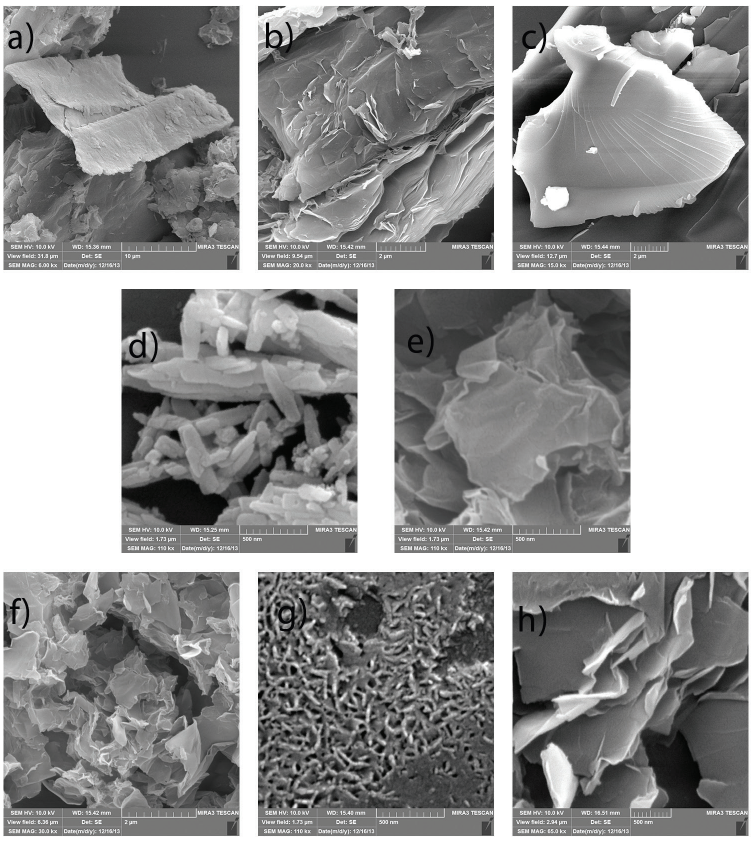

Figure 4. SEM images of (a) graphene and graphene modified by (b) pyridine-4-carboxylic acid, (c) thiophene-2-carbaldehyde, (d) thiophene-2-carboxylic acid, (e) hydrazine, (f) low-dose thiosemicarbazide, (g) high-dose thiosemicarbazide and (h) mercapto acetic acid [38–40].

http://dx.doi.org/10.5772/67490

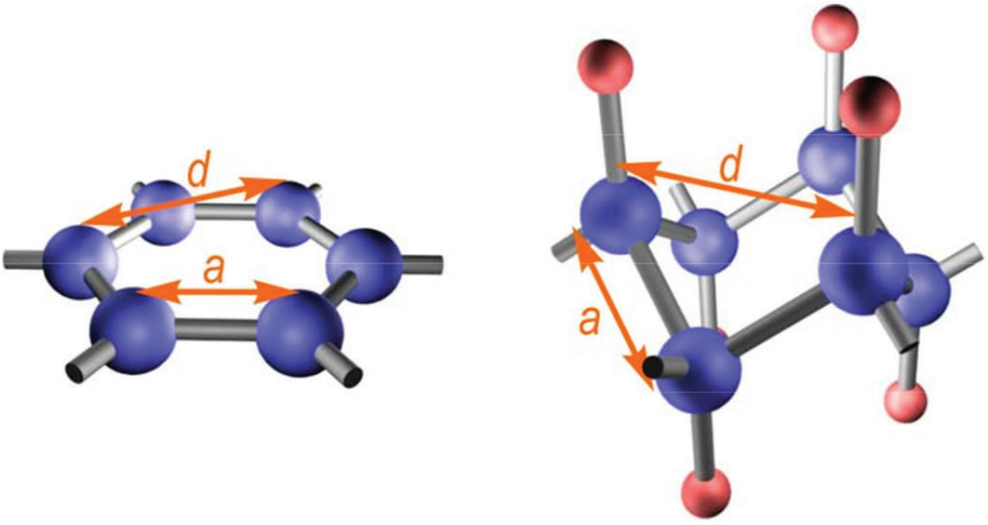

Figure 5. Scheme of out-of-plan distortion of graphene by hydrogenation process [45].

3.5. TEM

TEM images, which are shown in **Figure 6**, confirm this claim that the process of modification of graphene bended and finally rolled the sheets by revealing the detailed sub-structured information of the synthesized materials. **Figure 6(a)** shows unmodified graphene, which is almost uniform with some wrinkles. The TEM images of the graphene sheet modified low-dose thiosemicarbazide shown in **Figure 6 (b)**, which represent more wrinkles and bending in the sheet. **Figure 6(c)** is the TEM images of the high-dose-modified graphene sheet with thiosemicarbazide. It is obvious that thiosemicarbazide ligand completely rolled the sheet, and nanotubes with the diameter about 20 nm are achieved [40].

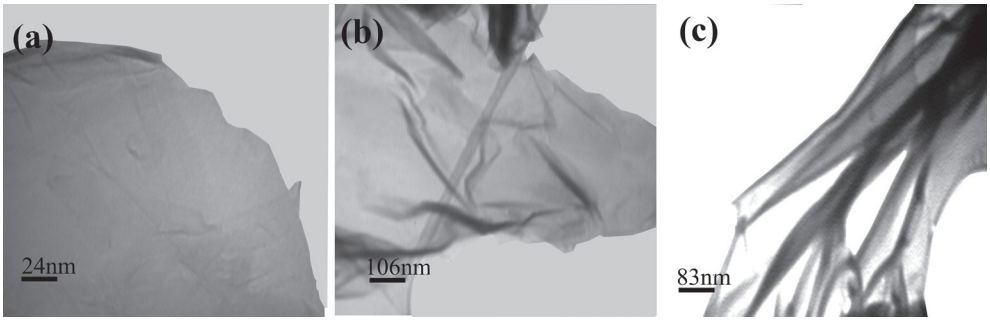

Figure 6. TEM image of (a) unmodified graphene, (b) modified by low-dose thiosemicarbazide and (c) modified by high-dose thiosemicarbazide [40].

3.6. AFM

Figure 7 shows the atomic force microscopy (AFM) topology images of the samples that confirm SEM and TEM results. The AFM images indicate that the organic ligands have well attached to the graphene sheet. With comparing of unmodified and modified graphene, one can conclude that the surface morphology of the graphene sheet become more and more uneven by applying organic ligands and using high concentration of them. Comparison of unmodified graphene with the reduced graphene oxide using high-dose hydrazine shows the height of wrinkles decreases [38]. This attributes to the removing of moisture trapped in the wrinkles in the course of chemical reduction of graphene oxide [40]. The surface of the nanorods, the result of modification of graphene with tiophene-2-carboxylic acid, which was seen in SEM images (see **Figure 4**), was also shown in AFM images [39].

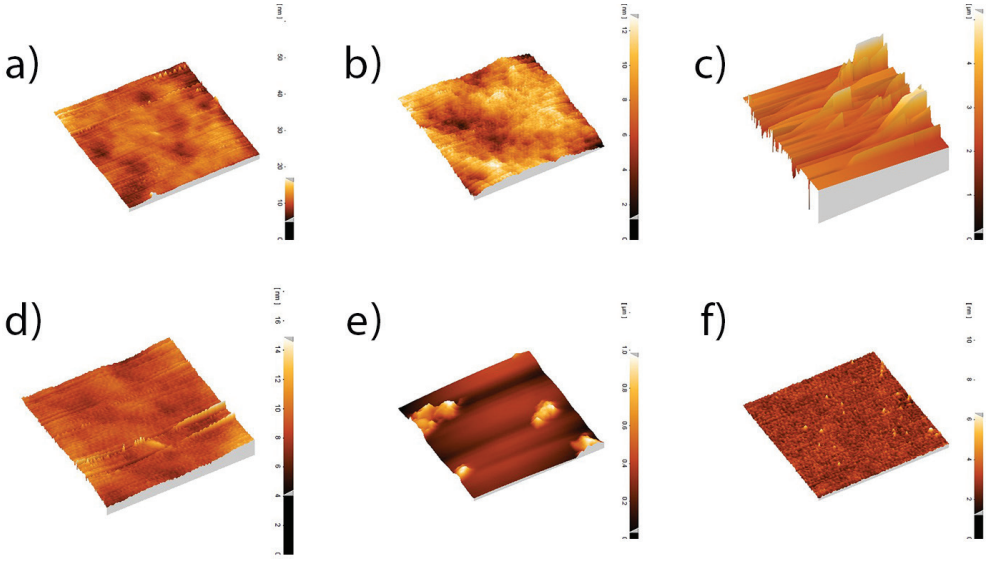

Figure 7. AFM image of (a) graphene (b) modified by low-dose thiosemicarbazide, (c) modified by high-dose thio semi carbazide, (d) modified by pyridine-4-carboxylic acid, (e) thiophene-2-carboxylic acid and (f) thiophene-2-carbaldehyde [38–40].

3.7. XRD

The powder X-ray diffraction (PXRD) patterns of the graphene oxide, unmodified and modified graphene are demonstrated in **Figure 8**. As illustrated in this figure, graphene oxide exhibits a strong and partly broad peak at $2\theta = 12.02°$ with an interlayer distance of 0.77 nm. Graphite flakes exhibit a strong and sharp peak at about $2\theta = 26°$, which indicate a higher order structure with an interlayer distance of 0.34 nm along the (002) orientation [46]. The comparison of XRD pattern of graphite with the graphene oxide reveals that the interlayer spacing of GO, which is about 0.77 nm, is higher than the interlayer space of the graphene

http://dx.doi.org/10.5772/67490

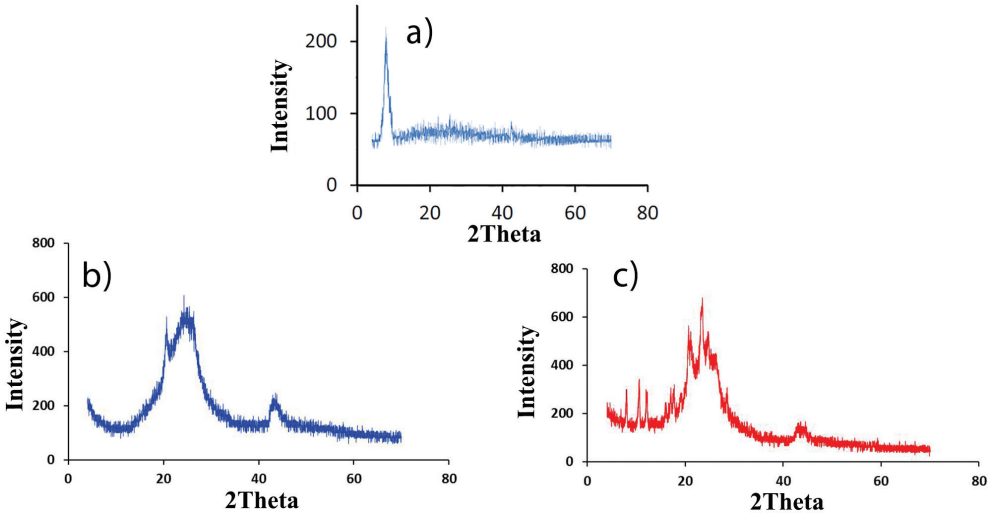

Figure 8. XRD patterns of (a) graphene oxide, (b) graphene and (c) graphene modified by thiosemicarbazide [38–40].

flakes because of the existence of oxygenated functional groups and intercalated water molecules in graphene oxide which are the result of chemical oxidation. In other words, graphene oxide is the graphene densely covered with hydroxyl and other groups [45]. By removing these groups from the surface of graphene sheet, graphene oxide XRD peak at $2\theta = 12°$ is diminished. This disappearance confirms the formation of graphene. The short range order in stacked stacks of graphene leads to the broadening of the characteristic diffraction peak of graphite. The XRD peak of graphene occurred at $2\theta = 24°$, which corresponds to an interlayer distance of 0.37 nm, is slightly shifted to the lower angles. The reason for this movement in XRD pattern stems from the remaining of trivial amount of residual oxygenated functional group or other structural defects [47, 48].

The XRD pattern of the modified graphene with thiosemicarbazide (see **Figure 8**) not only does show the slight shift to the left, but also indicates the new peaks appeared at lower angles. One possible rationale for this change is the creation of the new local thiosemicarbazide-graphene phase, which in turn could be an evidence for a structural chemical reaction between the free electrons of graphene and electrons of thiosemicarbazide to form a chemical bond, which results in the formation of new crystalline phase [40].

4. Simulation

Modifying surface of synthesized graphene with organic ligands dramatically increases the photosensitivity and significantly decreases the response time. In addition, shallow defects, an outgrowth of modification process, in electronic structure of graphene cause the improvement in responsivity compared to reported results [41]. Modification of graphene sheet with

ligands is occurred when the surface atoms of graphene interact with hydrogen atoms of organic ligands [40]. The formation of the defect electron trapping centres is the outcome of the surface modification (see **Figures 9–12**), which leads to band gap opening in electronic surface of hybrid material.

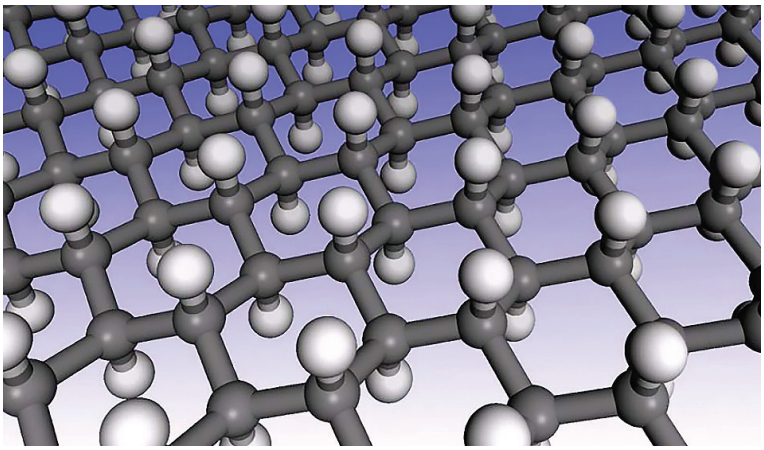

Figure 9. Scheme of graphane, fully hydrogenated graphene [37].

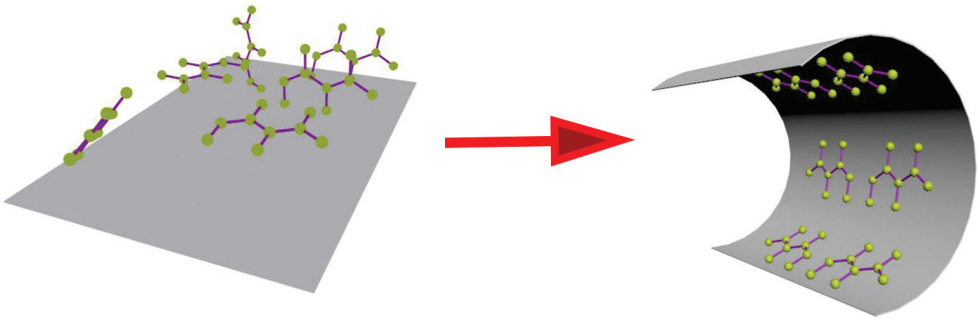

Figure 10. Schematic of rolling of graphene [40].

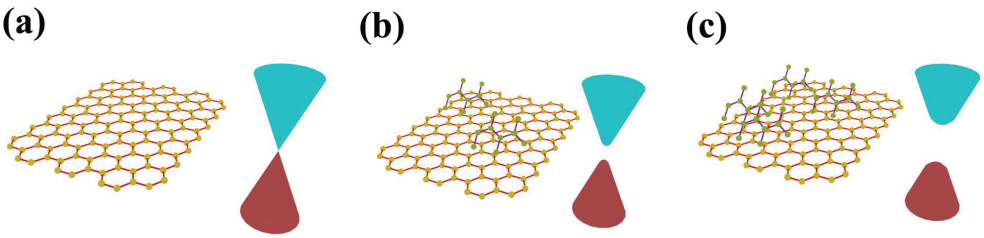

Figure 11. Schematic representation of band gap opening (a) unmodified graphene, (b) modified by low-dose thiosemicarbazide and (c) modified by high-dose thiosemicarbazide [41].

http://dx.doi.org/10.5772/67490

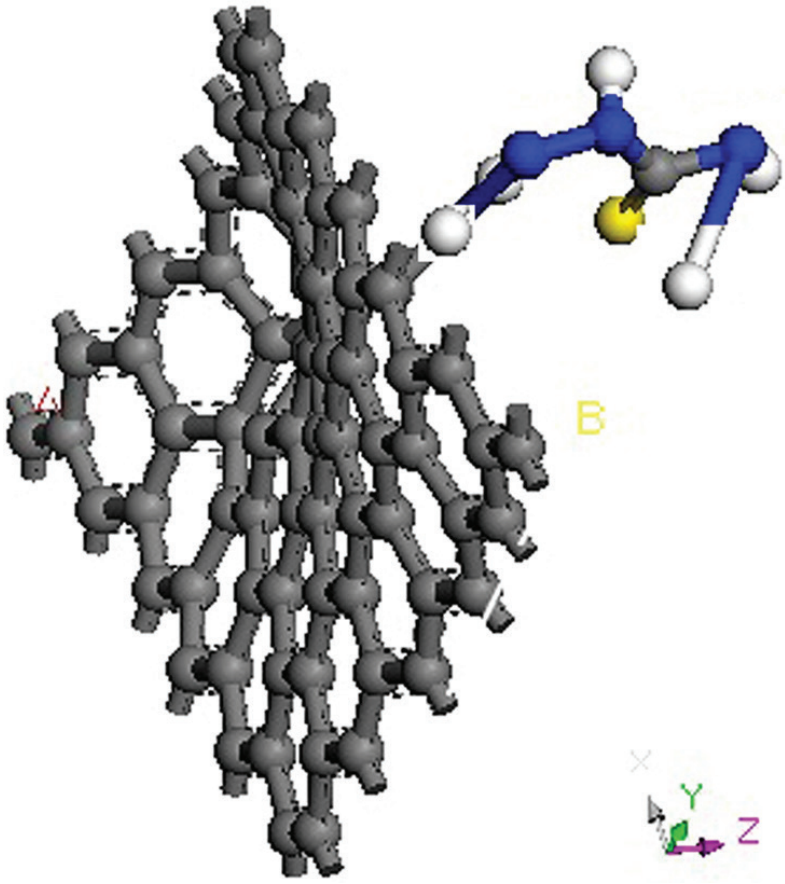

Figure 12. Schematic representation of band gap opening in the modified graphene [40].

DFT computations are executed to optimize the configuration of thiosemicarbazide adsorbed on graphene sheet [40]. The out-of-plane dislocation of graphene sheet, which is bonded to a thiosemicarbazide, is shown in **Figure 12**. As shown in this figure, the atomic dislocation of the graphene sheet is to be upward to hydrogen atoms of the organic ligand. The thiosemicarbazide is adhered to the graphene sheet via N-H aromatic π electron hydrogen bonding in which the thiosemicarbazide is a polar molecule [40].

DFT calculations indicate that the organic ligand can remarkably change the electronic state of graphene. Band length is changed due to the fact that hybridization of graphene change from sp^2 to sp^3 by attaching the hydrogen atoms to graphene sheet, which in turn leads to form the band gap. **Figure 13** shows the synthesized material behaves as a semiconductor with the band gap of 0.19 eV [40]. The significant part of the enhancement of the photo-sensitivity of graphene-based photodetector is a band gap creation in the band diagram of it.

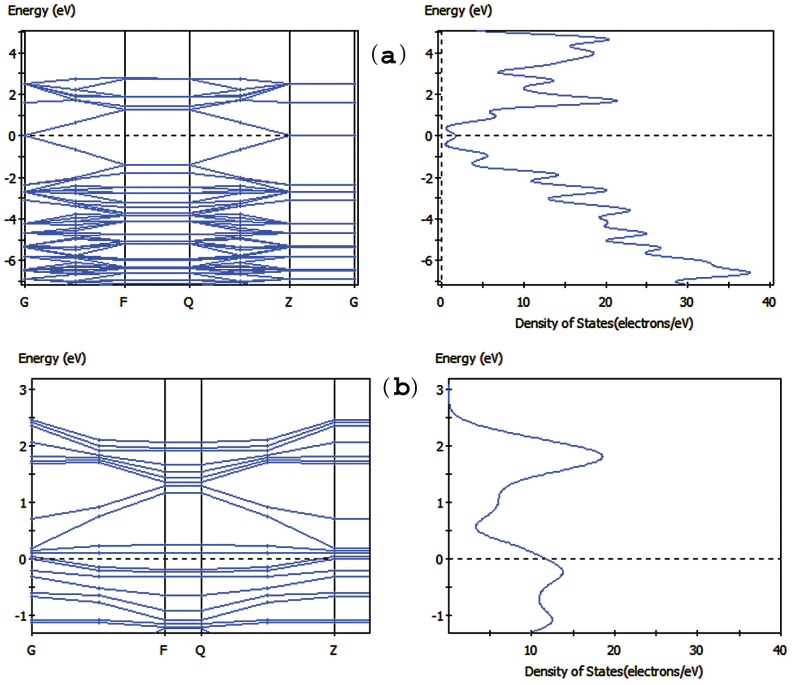

Figure 13. Calculated band structure and density of states for (a) graphene and (b) graphene modified by thiosemicarbazide [40].

5. Conclusion

In this work, graphene was efficiently prepared. The synthesized graphene was modified using different organic ligands. The chemical and structural properties of synthesized materials were investigated. Moreover, metal-graphene-metal (MGM) mid-IR photodetectors, in which the synthesized, modified and modified graphene used as an active layer, were fabricated and analysed at room temperature. The organic ligand used to modify graphene sheet can create and tune the band gap. Opening of the band gap overcomes the main weakness of graphene-based photodetectors such as high dark current, low sensitivity, repeatability and the effect of surrounding gases. Also, fast response time of fabricated photodetector reported that graphene-based photodetectors are the other benefits of our proposed structure.

Acronyms

SEM Scanning electron microscope

AFM Atomic force microscope

PXRD	Powder X-ray diffraction
TEM	Transmission electron microscope
MGM	Metal-graphene-metal
IR	Infrared
DOS	Density of states
LDA	Local density approximation
Ec	Cut-off energy
GO	Graphite oxide

Author details

Mehrdad Siahsar[1], Mahboubeh Dolatyari[2*], Ali Rostami[1,2] and Ghasem Rostami[2]

*Address all correspondence to: m.dolatyari@gmail.com

1 OIC Research Group, University of Tabriz, Tabriz, Iran

2 SP-EPT Labs, ASEPE Company, Industrial Park of Advanced Technologies, Tabriz, Iran

References

[1] K. S. Novoselov, A. K. Geim, S. V. Morozor, D. Jiang, Y. Zhang, S. V. Dubonos, I. V. Grigorieva, and A. A. Firsov. Electric Field Effect in Atomically Thin Carbon Films. Science. 2004;**306**:666–669.

[2] A. C. Ferrari, J. C. Meyer, V. Scardaci, C. Casiraghi, M. Lazzeri, F. Mauri, S. Piscanec, D. Jiang, K. S. Novoselov, and S. Roth. Raman Spectrum of Graphene and Graphene Layers. Phys. Rev. Lett. 2006;**97**(18):187401-1–187401-4.

[3] C. Popovici, C. S. Fischer, and L. von Smekal. Fermi Velocity Renormalization and Dynamical Gap Generation in Graphene. Phys. Rev. B. 2013;**88**(20):205429-1–205429-9.

[4] K. S. Novoselov, A. K. Geim, S. V. Morozov, D. Jiang, M. I. Katsnelson, I. V. Grigorieva, S. V. Dubonos, and A. A. Firsov. Two-Dimensional Gas of Massless Dirac Fermions in Graphene. Nature. 2005;**438**:197–200.

[5] Y. Liu, N. O. Weiss, X. Duan, H. Cheng, Y. Huang, and X. Duan. Van der Waals Heterostructures and Devices. Nat. Rev. Mater. 2016;**1**(9):16042.

[6] A. Varykhalov, J. Sãnchez-Barriga, A. Shikin, C. Biswas, E. Vescovo, A. Rybkin, D. Marchenko, and O. Rader. Electronic and Magnetic Properties of Quasifreestanding Graphene on Ni. Phys. Rev. Lett. 2008;**101**(15):157601-1–157601-4.

[7] Y. Wang, S. W. Tong, X. F. Xu, B. Özyilmaz, and K. P. Loh. Interface Engineering of Layer-by-Layer Stacked Graphene Anodes for High-Performance Organic Solar Cells. Adv. Mater. 2011;**23**(13):1514–1518.

[8] C. Soldano, A. Stefani, V. Biondo, L. Basiricò, G. Turatti, G. Generali, L. Ortolani, V. Morandi, G. P. Veronese, R. Rizzoli, R. Capelli, and M. Muccini. ITO-Free Organic Light-Emitting Transistors with Graphene Gate Electrode. ACS Photonics. 2014;**1**(10):1082–1088.

[9] D. Schall, D. Neumaier, M. Mohsin, B. Chmielak, J. Bolten, C. Porschatis, A. Prinzen, C. Matheisen, W. Kuebart, B. Junginger, W. Templ, A. L. Giesecke, and H. Kurz. 50 GBit/s Photodetectors Based on Wafer-Scale Graphene for Integrated Silicon Photonic Communication Systems. ACS Photonics. 2014;**1**(9):781–784.

[10] A. K. Geim and K. S. Novoselov. The Rise of Graphene. Nat. Mater. 2007;**6**(3):183–191.

[11] Y. Zhang, T. Liu, B. Meng, X. Li, G. Liang, X. Hu, and Q. J. Wang. Broadband High Photoresponse from Pure Monolayer Graphene Photodetector. Nat. Commun. 2013;**4**: 1811-1–1811-11.

[12] R. Zhang and R. Cheung. Mechanical Properties and Applications of Two-Dimensional Materials. In: Dr. Pramoda Nayak , editor. Two-dimensional Materials - Synthesis, Characterization and Potential Applications. Rijeka, Crotia: InTech; 2016. p. 219–246. DOI: 10.5772/64017

[13] A. M. Alexeev, M. D. Barnes, V. K. Nagareddy, M. F. Craciun, and C. D. Wright. A Simple Process for the Fabrication of Large-Area CVD Graphene Based Devices via Selective in Situ Functionalization and Patterning. 2D Mater. 2016;**4**(1):011010.

[14] Y. J. Kim, Y. Kim, K. Novoselov, and B. H. Hong. Engineering Electrical Properties of Graphene: Chemical Approaches. 2D Mater. 2015;**2**(4):042001.

[15] R. Vargas-Bernal. State-of-the-Art Electronic Devices Based on Graphene. In: Dr. Abhijit Kar, editor. Nanoelectronics and Materials Development. Rijeka, Crotia: InTech; 2016. p. 1–21. DOI: 10.5772/64320

[16] Y. D. Kim and M.-H. Bae. Light Emission from Graphene. In: Dr. Adrián Silva, editor. Advances in Carbon Nanostructures. Rijeka, Crotia: InTech; 2016. p. 83-100. DOI: 10.5772/64051

[17] G. Hwang, J. C. Acosta, E. Vela, S. Haliyo, and S. Régnier. Graphene as thin film infrared optoelectronic sensor. In: International Symposium on Optomechatronic Technology (ISOT); 2009; Istanbul, Turkey. IEEE; 2009. p. 169-174.

[18] G. Koley, A. Singh, and A. Uddin. Graphene-Based Sensors: Current Status and Future Trends. In: M. Aliofkhazraei, N. Ali, W. I. Milne, C. S. Ozkan, S. Mitura, and J. L. Gervasoni, editors. Graphene Science Handbook. Florida, USA: CRC Press; 2016. p. 211–234.

[19] Y.-W. Tan, Y. Zhang, K. Bolotin, Y. Zhao, S. Adam, E. H. Hwang, S. Das Sarma, H. L. Stormer, and P. Kim. Measurement of Scattering Rate and Minimum Conductivity in Graphene. Phys. Rev. Lett. 2007;**99**(24):246803-1–246803-4.

[20] M. Y. Han, B. Özyilmaz, Y. Zhang, and P. Kim. Energy Band-Gap Engineering of Graphene Nanoribbons. Phys. Rev. Lett. 2007;**98**(20):206805-1–206805-4.

[21] G. Guan, J. Lu, and H. Jiang. Preparation, Characterization, and Physical Properties of Graphene Nanosheets and Films Obtained from Low-Temperature Expandable Graphite. J. Mater. Sci. 2016;**51**(2):926–936.

[22] A. Celis, M. N. Nair, A. Taleb-Ibrahimi, E. H. Conrad, C. Berger, W. A. de Heer, and A. Tejeda. Graphene Nanoribbons: Fabrication, Properties and Devices. J. Phys. D: Appl. Phys. 2016;**49**(14):143001.

[23] Y. Zhang, T. Tang, C. Girit, Z. Hao, M. C. Martin, A. Zettl, M. F. Crommie, Y. R. Shen, and F. Wang. Direct Observation of a Widely Tunable Bandgap in Bilayer Graphene. Nature. 2009;**459**(7248):820–823.

[24] S. K. Jain, V. Juričić, and G. T. Barkema. Structure of Twisted and Buckled Bilayer Graphene. 2D Mater. 2016;**4**(1):015018.

[25] J. Zhou, M. M. Wu, X. Zhou, and Q. Sun. Tuning Electronic and Magnetic Properties of Graphene by Surface Modification. Appl. Phys. Lett. 2009;**95**(10):103108-1–103108-3.

[26] A. Nazari, R. Faez, and H. Shamloo. Modeling Comparison of Graphene Nanoribbon Field Effect Transistors with Single Vacancy Defect. Superlattices Microstruct. 2016;**97**:28–45.

[27] H. Li, Y. Zhou, and J. Dong. First-Principles Study of the Electron Transport Properties of Graphene-Like 2D Materials. In: A. Kar, editor. Nanoelectronics and Materials Development. InTech; 2016; p. 117–139. DOI: 10.5772/64109

[28] D. De Fazio, I. Goykhman, M. Bruna, A. Eiden, S. Milana, D. Yoon, U. Sassi, M. Barbone, D. Dumcenco, K. Marinov, and A. Kis. High Responsivity, Large-Area Graphene/MoS2 Flexible Photodetectors. ACS Nano. 2016;**10**(9):8252–8262.

[29] X. Wang, Z. Cheng, K. Xu, H. K. Tsang, and J. B. Xu. High-Responsivity Graphene/Silicon-Heterostructure Waveguide Photodetectors. Nat. Photonics. 2013;**7**(11):888–891.

[30] N. Jain, and B. Yu. Graphene-Enabled Heterostructures: Role in Future-Generation Carbon Electronics. In: M. Aliofkhazraei, N. Ali, W. I. Milne, C. S. Ozkan, S. Mitura, and J. L. Gervasoni, editors. Graphene Science Handbook. Florida, USA: CRC Press; 2016. p. 423–434.

[31] K. S. Novoselov, A. Mishchenko, A. Carvalho, and A. H. Castro Neto. 2D materials and van der Waals heterostructures. Science. 2016; **353**(6298): aac9439.

[32] D. Jariwala, T. J. Marks, and M. C. Hersam. Mixed-dimensional van der Waals heterostructures. Nat. Mater. 2017; 16: 170–181.

[33] H. Talebi, M. Dolatyari, G. Rostami, A. Manzuri, M. Mahmudi, and A. Rostami. Fabrication of Fast Mid-Infrared Range Photodetector Based on Hybrid Graphene-PbSe Nanorods. Appl. Opt. 2015;**54**(20):6386–6390.

[34] J. J. Navarro, S. Leret, F. Calleja, D. Stradi, A. Black, R. Bernardo-Gavito, M. Garnica, D. Granados, A. L. Vázquez de Parga, E. M. Pérez, and R. Miranda. Organic Covalent Patterning of Nanostructured Graphene with Selectivity at the Atomic Level. Nano Lett. 2016;**16**(1):355–361.

[35] G. Konstantatos, M. Badioli, L. Gaudreau, J. Osmond, M. Bernechea, F. P. Garcia de Arquer, F. Gatti, F. H. L. Koppens. Hybrid Graphene-Quantum Dot Phototransistors with Ultrahigh Gain. Nat. Nanotechnol. 2012;**7**:363–368.

[36] S. Mitra, S. Banerjee, A. Datta, and D. Chakravorty. A Brief Review on Graphene/Inorganic Nanostructure Composites: Materials for the Future. Indian J. Phys. 2016;**90**(9):1019–1032.

[37] J. O. Sofo, A. S. Chaudhari, and G. D. Barber. Graphane: A Two-Dimensional Hydrocarbon. Phys. Rev. B. 2007;**75**(15):153401.

[38] F. Jabbarzadeh, M. Siahsar, M. Dolatyari, G. Rostami, and A. Rostami. Modification of Graphene Oxide for Applying as Mid-Infrared Photodetector. Appl. Phys. B. 2015;**120**:637–643.

[39] F. Jabbarzadeh, M. Siahsar, M. Dolatyari, G. Rostami, and A. Rostami. Fabrication of New Mid-Infrared Photodetectors Based on Graphene Modified by Organic Molecules. IEEE Sens. J. 2015;**15**:2795–2800.

[40] M. Siahsar, F. Jabbarzadeh, M. Dolatyari, G. Rostami, and A. Rostami. Fabrication of High Sensitive and Fast Response MIR Photodetector Based on a New Hybrid Graphene Structure. Sens. Actuators A. 2016;**238**:150–157.

[41] W. J. Yu, Z. Li, H. Zhou, Y. Chen, Y. Wang, Y. Huang, and X. Duan. Vertically Stacked Multi-Heterostructures of Layered Materials for Logic Transistors and Complementary Inverters. Nat. Mater. 2012;**12**(3):246–252.

[42] Y. J. Kim, Y. H. Kahng, N. Kim, J. H. Lee, Y. H. Hwang, S. M. Lee, S. M. Choi, W. B. Kim, and K. Lee. Impact of Synthesis Routes on the Chemical, Optical, and Electrical Properties of Graphene Oxides and Its Derivatives. Curr. Appl. Phys. 2015;**15**(11):1435–1444.

[43] S. Bykkam, K. V. Rao, C. H. S. Chakra, and T. Thunugunta. Synthesis and Characterization of Graphene Oxide and Its Antimicrobial Activity Against Klebseilla and Staphylococus. Int. J. Adv. Biotechnol. Res. 2013;**4**(1):142–146.

[44] Y. Liu, R. Cheng, L. Liao, H. Zhou, J. Bai, G. Liu, L. Liu, Y. Huang, and X. Duan. Plasmon Resonance Enhanced Multicolour Photodetection by Graphene. Nat. Commun. 2011;**2**:579.

[45] D. C. Elias, R. R. Nair, T. M. G. Mohiuddin, S. V. Morozov, P. Blake, M. P. Halsall, A. C. Ferrari, D. W. Boukhvalov, M. I. Katsnelson, A. K. Geim, and K. S. Novoselov. Control of Graphene's Properties by Reversible Hydrogenation: Evidence for Graphane. Science. 2009;**323**(5914):610–613.

[46] S. Thakur and N. Karak. Green Reduction of Graphene Oxide by Aqueous Phytoextracts. Carbon. 2012;**50**(14):5331–5339.

[47] S. Park, J. An, I. Jung, R. D. Piner, S. J. An, X. Li, A. Velamakanni, and R. S. Ruoff. Colloidal Suspensions of Highly Reduced Graphene Oxide in a Wide Variety of Organic Solvents. Nano Lett. 2009;**9**(4):1593–1597.

[48] D. Li, M. B. Müller, S. Gilje, R. B. Kaner, and G. G. Wallace. Processable Aqueous Dispersions of Graphene Nanosheets. Nat. Nanotechnol. 2008;**3**:101–105.